

# INTERNATIONAL SOCIETY FOR SOIL MECHANICS AND GEOTECHNICAL ENGINEERING



*This paper was downloaded from the Online Library of the International Society for Soil Mechanics and Geotechnical Engineering (ISSMGE). The library is available here:*

<https://www.issmge.org/publications/online-library>

*This is an open-access database that archives thousands of papers published under the Auspices of the ISSMGE and maintained by the Innovation and Development Committee of ISSMGE.*

*The paper was published in the proceedings of the 20<sup>th</sup> International Conference on Soil Mechanics and Geotechnical Engineering and was edited by Mizanur Rahman and Mark Jaksa. The conference was held from May 1<sup>st</sup> to May 5<sup>th</sup> 2022 in Sydney, Australia.*

## Spectral-analysis-of-body-waves (SABW) method for crosshole seismic testing

Méthode d'analyse spectrale des ondes corporelles (SABW) pour les tests sismiques en trou croisé

**Sungmoon Hwang**

*Civil, Architectural and Environmental Engineering, USA, syongmoon@utexas.edu*

**Kenneth H. Stokoe II**

*Civil, Architectural and Environmental Engineering, USA, k.stokoe@mail.utexas.edu*

**ABSTRACT:** Crosshole seismic testing is commonly used to determine detailed and reliable compression- and shear-wave velocity profiles. The conventional crosshole analysis method requires picking a first arrival point on time-domain waveforms from which travel times between the source and receiver in one or more boreholes are calculated. Since the crosshole source is located at the same depth as the receiver(s), wave velocities are simply calculated by dividing the travel distance between the measurement points by the travel times. There are, however, two shortcomings in this conventional time-domain analysis method. First, selecting reference points by visual selection can be subjective which can limit precision and increase variability of the wave velocity calculation. Second, the conventional crosshole analysis method ignores dispersion in body waves. To remove the subjectivity of visual selections of arrival times and to investigate the impact of dispersion of body waves, the Spectral-Analysis-of-Body-Waves (SABW) method is presented herein. A reliable framework for calculating the correct wave velocities using the SABW method is also proposed which includes waveform segmentation and pseudo-triggering.

**RÉSUMÉ :** Les tests sismiques en trou croisé sont couramment utilisés pour déterminer des profils de vitesse d'onde de compression et de cisaillement détaillés et fiables. La méthode d'analyse crosshole conventionnelle nécessite de choisir un premier point d'arrivée sur des formes d'onde dans le domaine temporel à partir desquelles les temps de trajet entre la source et le récepteur dans un ou plusieurs forages sont calculés. Étant donné que la source crosshole est située à la même profondeur que le ou les récepteurs, les vitesses des ondes sont simplement calculées en divisant la distance de déplacement entre les points de mesure par les temps de déplacement. Il y a, cependant, deux lacunes dans cette méthode conventionnelle d'analyse dans le domaine temporel. Premièrement, la sélection de points de référence par sélection visuelle peut être subjective, ce qui peut limiter la précision et augmenter la variabilité du calcul de la vitesse des ondes. Deuxièmement, la méthode conventionnelle d'analyse des trous croisés ignore la dispersion des ondes corporelles. Pour supprimer la subjectivité des sélections visuelles des temps d'arrivée et pour étudier l'impact de la dispersion des ondes corporelles, la méthode Spectral-Analysis-of-Body-Waves (SABW) est présentée ici. Un cadre fiable pour calculer les vitesses d'onde correctes à l'aide de la méthode SABW est également proposé, qui comprend la segmentation de la forme d'onde et le pseudo-déclenchement.

**KEYWORDS:** crosshole seismic testing, spectral-analysis-of-body-waves, dispersion in body waves, segmentation, pseudo-trigger

### 1 INTRODUCTION

In-situ seismic testing is commonly used in geotechnical engineering to determine the wave velocity profiles of body waves, constrained compression (P) and shear (S) waves. Since body wave velocities are directly linked to elastic moduli of the geotechnical material, various in-situ seismic testing methods have been developed. There are two basic types of in-situ seismic testing methods, noninvasive surface-based methods, and invasive borehole-based methods. Noninvasive methods generally involve measuring Rayleigh-type surface waves, or direct, and/or refracted body waves while receivers are located on the ground surface. On the other hand, invasive methods require pre-drilled boreholes or pushing mechanisms to locate receivers below the ground surface. Invasive borehole-based methods were developed and extensively used in geophysics for oil exploration and were adapted in the 1970's (Stokoe & Woods 1972, Woods 1978, and Stokoe & Hoar 1978) for geotechnical engineering purposes. The seismic cone penetration test (SCPT) was first proposed by Stokoe and developed by Robertson et al. (1986) which combines the pushing mechanism of CPT equipment to advance the receiver into the ground instead of drilling the borehole. Among the various in-situ, invasive seismic testing, the crosshole, downhole and SCPT tests are the most widely used methods today in geotechnical earthquake engineering.

To analyze the seismic data collected from invasive seismic testing, a first arrival or common reference point on time-domain waveforms is visually identified. The wave velocities are calculated from the slopes of lines drawn through groups of waveforms with reference points that cover various depth ranges or from the time interval between reference points at different depths. There are, however, two shortcomings in this time-domain analysis method to determine wave velocities. First, selecting reference points by visual "picks" can be subjective for reasons such as signal clarity, mechanical and electrical interferences, and significant attenuation in the waveforms with depth. These factors can create inconsistencies and errors in arrival-time selections which affect the wave velocity calculation. Second, dispersion of body waves is not considered in calculating wave velocities; that is different frequencies propagate with different velocities and attenuate at different rates in uniform and layered geological materials. To overcome these limitations, the Spectral-Analysis-of-Body-Waves (SABW) method is introduced in this study. The SABW method was proposed by Kim (2012) and improved by Hwang (2018). To correctly calculate the wave velocities using the SABW method, a reliable framework is proposed which includes waveform segmentation and pseudo-triggering.

The SABW method can be applied to all invasive seismic testing methods in which time-domain waveforms are recorded. The SABW method uses the phase-difference between source to receiver and receiver pairs to evaluate the travel time at each

frequency. Once travel time is evaluated, the wave velocity is calculated by dividing the travel path by the travel time. In the case of crosshole testing where the source and receivers are located at same depth, the application of the SABW method is simple since the horizontal travel path can be represented by the distance between the source and/or receivers (when the distance between receivers are close enough to eliminate any possibility of refracted waves) and the generated wave is normally propagating in a single layer. Therefore, the SABW method is illustrated and explained using crosshole seismic data which normally does not require consideration of a complex wave travel path.

The SABW method is theoretically verified using synthetic waveforms and laboratory experiments. Two sets of crosshole seismic data are analyzed using the SABW method and are compared with conventional analysis result. Two sets of crosshole test were performed, one at a backfill test pad and the second at a Hornsby Bend Research Site operated by the University of Texas at Austin with permission from the city of Austin, Texas. The compacted backfill test pad represents a site with small velocity contrast in the Vs profile, and the Hornsby Bend Research site represents a site with large velocity contrast in the Vs profile.

## 2 SPECTRAL ANALYSIS OF BODY WAVES

The most explicit way to calculate wave velocity from measurements with a receiver pair is to divide the distance by the travel time between the receivers. Since the distance can normally be measured, the travel time is the key factor in calculating the velocity, and the travel time can be evaluated from the phase difference between the receiver pair. If the wave with a frequency of  $f_0$  propagates from locations A to B with the travel time of  $t_1$ , the wave motion at locations A and B can be expressed in time difference by the following equations for  $y_1$  and  $y_2$  as shown in Figure 1.

$$\begin{aligned} y_1 &= \sin(2\pi f_0 t), & (1) \\ y_2 &= \sin[2\pi f_0 (t - t_1)], & (2) \\ y_2 &= \sin[2\pi f_0 t - 2\pi f_0 t_1]. & (3) \end{aligned}$$

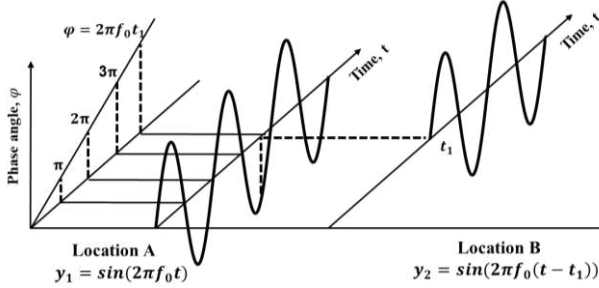


Figure 1. Illustration of phase difference between two waveforms at locations A and B (after Joh, 1996)

On the other hand, the wave motion at location B can also be expressed in phase difference by the following equation:

$$y_2 = \sin[2\pi f_0 t - \varphi] \quad (4)$$

where  $\varphi$  is the phase difference between the two locations, A and B, propagating with frequency of  $f_0$ . Since Eqs. 3 and 4 express the wave motion at the same location of B, the two equations should be equal to each other. Therefore, the phase difference and the travel time can be related as:

$$\varphi = 2\pi f_0 t_1 \quad (5)$$

which is,

$$t_1 = \frac{\varphi}{2\pi f_0} \quad (6)$$

By using Eq. 6, the travel time between the two receiver locations can be evaluated with the phase difference at a single

frequency  $f_0$ . As a result, phase velocity at a single frequency  $f_0$ ,  $V_{PH}$ , can be calculated by dividing the distance  $d$  with  $t_1$  which is:

$$V_{PH} = \frac{d}{t_1}, \quad (7)$$

$$V_{PH} = \frac{2\pi f_0}{\varphi} \times d, \quad (8)$$

$$V_{PH} = f_0 \times \frac{360^\circ}{\varphi} \times d. \quad (9)$$

In short, phase velocity can be calculated with the distances between source and receiver and/or two receivers,  $d$ , the phase difference between these two points,  $\varphi$ , and the corresponding frequency,  $f$ . This process of calculating the phase velocity associated with the frequency is called the phase difference method, and the SABW method utilizes this method to calculate the wave velocities at each frequency. Generally, the phase difference between two receivers is obtained using the transfer function of the Fourier transform or the cross-power spectrum.

## 3 THE PROPOSED FRAMEWORK

There are four requirements to correctly calculate the wave velocities using the SABW method. These requirements are: (1) a single wave group, (2) a frequency of local maxima, (3) a maximum amplitude at the first peak arrival, and (4) a proper trigger. The major steps to accomplish these four requirements are summarized in Figure 2. The synthetic time record shown in Figure 3 was created and processed by following flow chart to demonstrate how the process affects the wave velocity calculation.

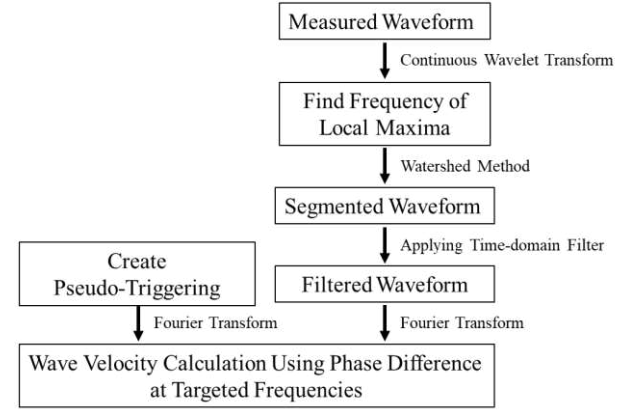


Figure 2. A flow chart of the proposed framework

### 3.1 Synthetic waveform

With reference to Figure 3, a synthetic waveform is created by adding the later arrival of a wave group to a 45-degree phase shift, 500 Hz, 20 cycles sinusoidal wave. The arrival time of the first wave group is 0.01 sec, the arrival time of the second wave group is 0.026 sec with the distance between the source and the receiver is 2 m indicating a wave velocity of 200 m/sec.

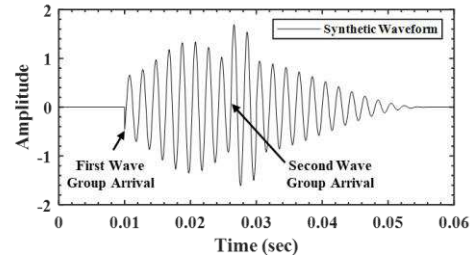


Figure 3. Synthetic waveform with two, wave-group arrivals

### 3.2 Segmentation

To obtain the correct wave velocity, the first step is to segment the synthetic waveform to have a single wave group. In this step,

the time-domain waveform is converted to the time-frequency domain by applying the continuous wavelet transform as shown in Figure 4a. The segmentation is done by using the watershed algorithm (Meyer 1994) and the frequency of the local maxima.

The Matlab function *watershed* was employed to segment the synthetic wave which uses the Meyer (1994) algorithm based on immersion simulations. The vertical boundary line is determined from a coordinate where the watershed line intercepts with the frequency of the local maxima (500 Hz) as shown in Figure 4a. The portion of the first wave group, the left portion from the vertical boundary line, is then converted to the time-domain by using inverse continuous wavelet transform as shown in Figure 4b with the blue line waveform between 0.01 and 0.026.

Once the spectral analysis method is applied to the segmented waveform, the phase angle at each frequency is calculated as shown in Figure 4c. The wrapped phase angle associated with the 500-Hz signal is 135 degrees as shown in Figure 4c by the red star which results in an unwrapped phase angle of 4,455 degrees.

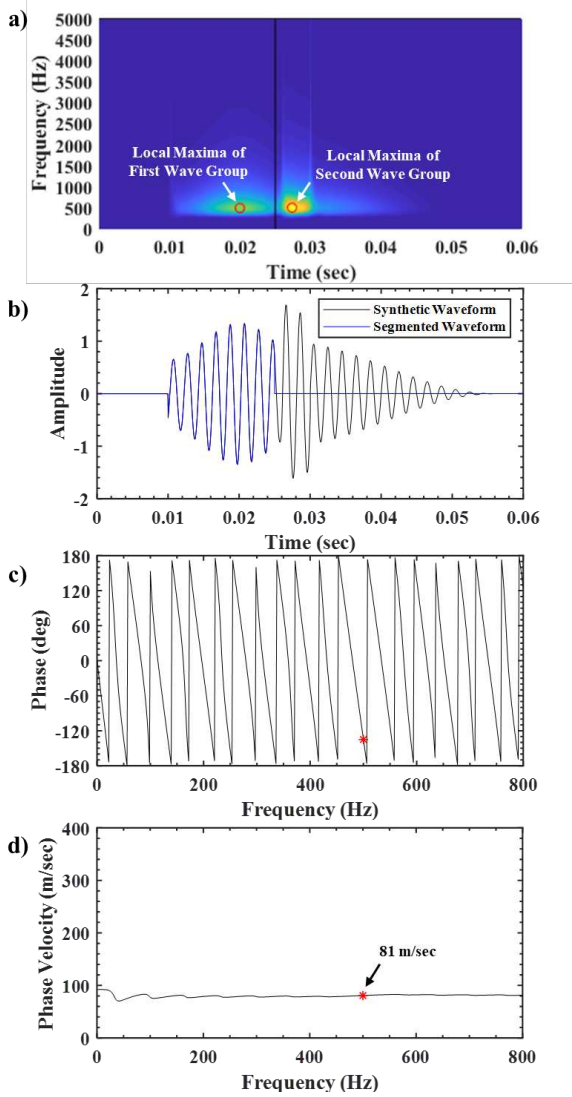


Figure 4. a) Continuous wavelet transform of the synthetic waveform and segmentation result using the watershed method, b) Comparison between the synthetic and segmented waveforms, c) Phase spectrum of the segmented waveform, and d) Phase velocity calculated using the phase spectrum of the segmented waveform

The phase velocity associated with 500 Hz is calculated using Eq 9, which is 81 m/sec as shown in Figure 4d.

The spectral analysis of the segmented waveform underestimates the wave velocity by 60 %; that is, because an additional cycle of phase occurred due to the group wave. To

remove the group wave interference, a window function is necessary.

### 3.3 Window function

To remove the interference of the group wave, a window function is applied to the segmented waveform. This window function is represented by Eq. 10 and graphically presented in Figure 5a as:

$$f(n) = \begin{cases} 1, & 1 \leq n < P_l \\ \frac{1}{2} \left( \cos \frac{n - P_l}{L_l} \pi + 1 \right), & P_l \leq n < P_l + L_l \\ 0, & P_l + L_l < n < N \end{cases} \quad (10)$$

Where  $P_l$  is the initial point of the transition band,  $L_l$  is the length of the cosine-tapered window, and  $N$  is the total number of points. This window function was designed by Joh (1996) to investigate the effect of different wave groups that are caused by

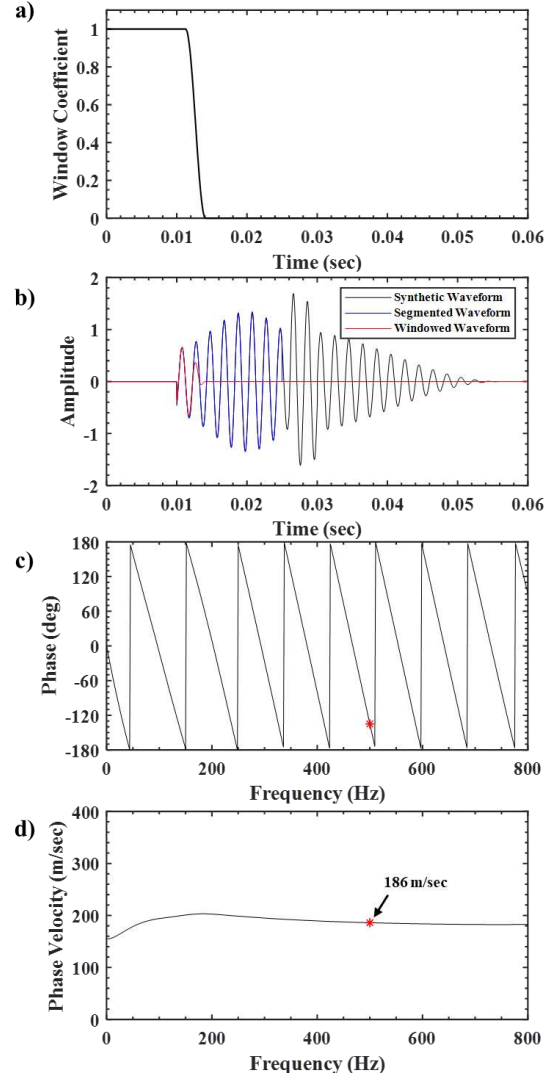


Figure 5. a) Window coefficient applied to the segmented waveform, b) Comparison between the synthetic, segmented, and windowed waveforms, c) Phase spectrum of the windowed waveform, and d) Phase velocity calculated using phase spectrum of the windowed waveform

refraction and/or reflection of stress waves at the interface between layers. This window maintains the earlier arrival of the waveform and minimizes the amplitude of the later arrival of the waveform. The  $P_l$  is set to an end of the first positive half cycle and the  $L_l$  is extended until the amplitude of the first peak remained as a maximum absolute value in Eq. 10. In the case of having a low signal-to-noise-ratio, a symmetrical window



function is necessary. More detailed information will be discussed in future publication due to space limitations. The window function is shown in Figure 5a is applied by multiplying the window coefficients times the segmented waveform as shown in 5b with the red line.

Once the spectral analysis method is applied to the windowed waveform, the phase angle at each frequency is calculated as shown in Figure 5c. The wrapped phase angle associated with 500-Hz signal is 135 degrees as shown in Figure 5c by the red star which results in an unwrapped phase angle of 1935 degrees. The phase velocity associated with 500 Hz is 186 m/sec as shown in Figure 5d. The additional cycle of phase around 50, 150, 250, 350, 450, 550, 650, 750 Hz are removed by applying the window function. In this case, the phase velocity is still underestimated by 7%.

### 3.4 Pseudo-Triggering

The final step in correcting the wave velocity calculation in the SABW method is to create a pseudo-triggering. The phase of the waveform calculated from the Fourier transform is the same as calculating the phase difference between the waveform and 0-degree phase signals at each frequency. In the perspective of a trigger signal in a time-domain record, it indicates that the trigger signal occurred at a negative time. This negative trigger time is the reason why the phase velocity calculated from the windowed waveform underestimates the value of wave velocity.

The pseudo-triggering created by using Eq. 11 is:

$$\sum_{f=1}^n \sin(2 * \pi * f * t) \quad (11)$$

in which  $n$  is target frequency and  $t$  is time.  $n$  is set to the target frequency instead of the Nyquist frequency due to the efficiency of coding. This trigger is equivalent to the waveform which has a constant amplitude in the frequency domain up to the target frequency with a 90-degree phase shift, meaning each frequency of the waveform trigger at 0 second. However, the wave velocity calculated from the phase difference between the windowed waveform and the pseudo-triggering will still underestimate the values since the synthetic waveform was designed with a 45 phase shifts.

The phase shift of the waveform is estimated using Matlab function *findchangepts* which use the sum of squared differences between the data points and the predicted least-squares linear fit through those points to detect the most abrupt changes in the waveform. In the case of the synthetic waveform where the arrival of the wave is apparent, the *findchangepts* can measure the exact phase shift as shown in Figure 6. However, in the case of measured waveforms, the *findchangepts* function is the best estimate of determining the arrival of the waveform which can also be used as a reference point for the time-domain analysis.

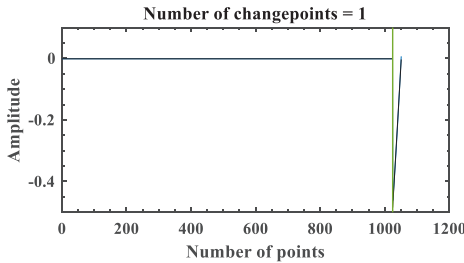


Figure 6. Matlab function *findchangepts* applied to the arrival of a windowed waveform

Once the estimated phase shift is included in the pseudo-triggering using Eq. 12, the phase velocity is correctly calculated using the phase difference between the pseudo-triggering and the windowed waveform. The equation representing this trigger is

$$\sum_{f=1}^n \sin(2 * \pi * f * t - \Delta t * k * 2 * \pi * f * t) \quad (12)$$

where  $\Delta t$  is the time difference between points and the value of  $k$  is the number of points between the most abrupt change and the zero amplitude of the waveform. The graphical form of the pseudo-triggering is shown in Figure 7a by the green line. The phase difference between the windowed waveform and the pseudo-triggering is calculated from the transfer function of the Fourier transform as shown in Figure 7b. The wrapped phase angle associated with the 500-Hz signal is 0 degree as shown in Figure 7b by the red star which results in an unwrapped phase angle of 1800 degrees. The phase velocity associated with 500 Hz is 200 m/sec as shown in Figure 7c which was originally designed. To study the dispersion of the body wave, the phase velocity associated with the frequency range of interest can be determined from Figure 7c.

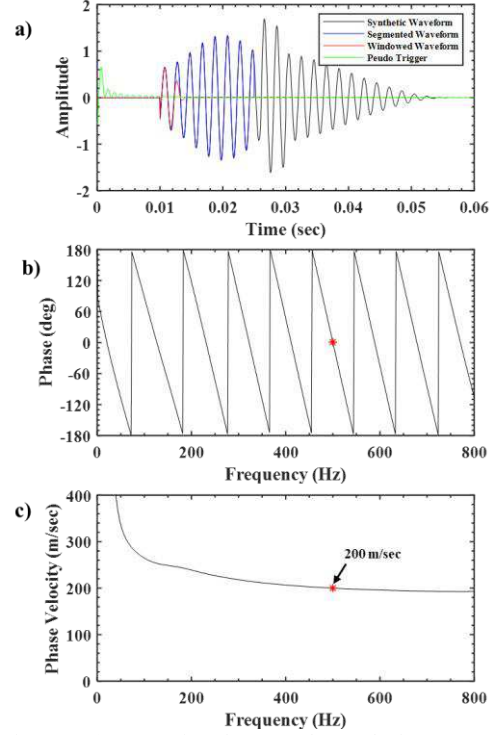


Figure 7. a) Comparison between the synthetic, segmented, windowed waveforms, and pseudo-triggering, b) Phase spectrum calculated between windowed waveform and pseudo-triggering, and c) Phase velocity calculated using phase spectrum between windowed waveform and pseudo triggering

## 4 LABORATORY EXPERIMENT

A controlled laboratory experiment enables verification of the SABW method with the known value of the wave velocity of the material. The unconfined, free-free, resonant column (URC) test was performed with an aluminum specimen. The URC test is a simple and accurate test to evaluate material stiffnesses and material damping ratios of soil and rock specimens at small strains. The simplicity of the free-free URC set-up is shown in Figure 8a. This simplicity eliminates potential compliance problems such as fixity of the bottom platen in a fixed-free configuration and equipment-induced damping in a torsional electrical motor (Stokoe et al, 1994).

In the free-free URC test, three body wave velocities can be evaluated. These wave velocities are: (1) unconstrained compression wave velocity ( $V_c$ ), (2) constrained compression wave velocity ( $V_p$ ), and (3) shear wave velocity ( $V_s$ ). With the relationships between those velocities, three values of Poisson's ratios can also be evaluated. In the URC test, measurement of the compressional and torsional resonant frequency of the specimen are used calculate the wave velocity using Eq. 13:

$$V = f_r * \lambda = f_r * 2 * l \quad (13)$$

where  $f_r$  is the first-mode resonant frequency of the specimen,  $\lambda$  is wavelength and  $l$  is the length of the specimen. The wavelength of specimens in the free-free boundary condition is simply twice the length of the specimen. To verify the proposed SABW method, the shear wave velocity of an aluminum specimen was calculated from the SABW method and compared with the value determined by the URC test evaluated using the first-mode torsional resonant frequency. To have a higher sampling frequency for higher resolution in the time-domain, an oscilloscope that has a one million Hz sampling rate with 2500 data points was used. For the URC test, a four-channel dynamic signal analyzer was used with a 200,000 Hz sampling rate with 130,000 data points.

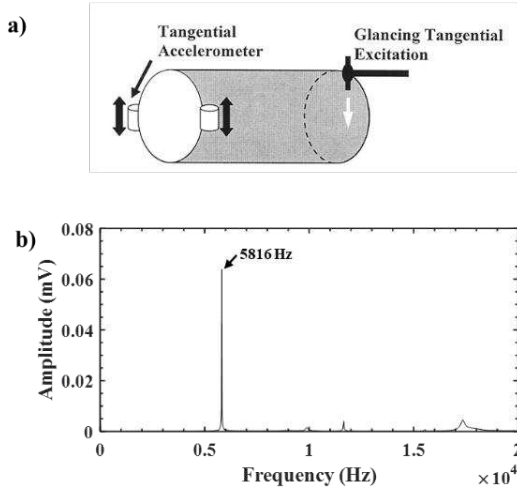


Figure 8. a) URC test set-up for torsional resonance testing, and b) Power spectrum of the aluminum specimen

The length of the aluminum specimen was 26.65 cm. The torsional resonant frequency was 5816 Hz as shown in Figure 8b. The shear wave velocity of the aluminum specimen was calculated using Eq. 13, and that was 3099 m/sec. The proposed SABW method was also applied to the shear waveform measured from the aluminum specimen. The continuous wavelet transform of the shear waveform and the segmentation using the watershed method is shown in Figure 9a. The frequency of the local maxima was 16276 Hz. The first arrival of the shear waveform traveling from the right end of the specimen where the tangential excitation was created to the other end where the tangential accelerometers were attached to measure the shear wave arrival is shown in Figure 8a. The travel distance equal to the length of the aluminum specimen which was 26.65 cm. The wrapped phase angle associated with the 16276-Hz signal was 143.67 degrees as shown in Figure 9c by the red star which results in an unwrapped phase of 503.67 degrees. The phase velocity associated with the 16276 Hz is 3100 m/sec as shown in Figure 9.d which is almost the same as the URC test result. The shear wave velocity of the aluminum specimen also can be calculated from the reference point of the most abrupt change in the waveform which results in the value of 3211 m/sec.

Furthermore, the SABW method can be applied to multiple arrivals of the windowed waveform. The second arrival of the shear waveform traveled from one end to the other end and back until the waveform propagates to the accelerometer. This

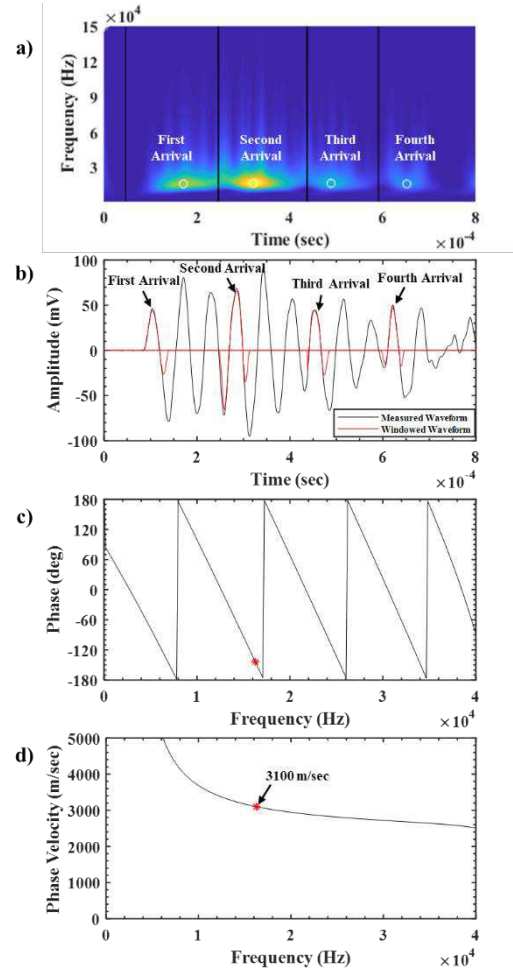


Figure 9. a) Continuous wavelet transform of the shear waveform measured from the aluminum specimen and the segmentation result using watershed method, b) Comparison between measured shear waveforms and windowed waveforms of multiple arrivals, c) Phase spectrum calculated between windowed waveforms of the first arrival and pseudo-triggering, and d) Phase velocity calculated using the phase spectrum between windowed waveform of the first arrival and pseudo triggering

distance is equal to three times the length of the aluminum specimen. The third arrival of the shear waveform travels five times of the length of the aluminum specimen and the Fourth arrival of the shear waveform travel seven times of the length of the aluminum specimen. Since the travel distances of the waveforms are determined, the phase wave velocities are calculated using the SABW method and the reference point of the most abrupt change in the waveform as shown in Table. 1.

The shear wave velocity calculated from the SABW method is closer to the value of 3099 m/sec which was evaluated from the URC test as shown in Table. 1. More importantly, the shear wave velocity calculated from the SABW method is more stable, with smaller variances compared to the velocity calculated from the reference points (time-domain analysis method).

Table 1. Shear wave velocities calculated using the SABW method and the reference point of the most abrupt change in the waveform

	First Arrival	Second Arrival	Third Arrival	Fourth Arrival
S-wave velocity from the SABW method (m/sec)	3100	3075	3076	3090
S-wave velocity from the reference point (m/sec)	3211	3075	3042	3068

## 5 FIELD TESTS

To evaluate the reliability of the proposed SABW method, crosshole data from two sites, a compacted backfill test pad and Hornsby Bend Research site, are analyzed using the SABW method and are compared with results from the conventional time-domain analysis method.

As part of a subsurface characterization program of a potential site for two nuclear power plants, a compacted backfill test pad was constructed. The objective of the test-pad construction was to assess the potential of on-site granular soils for fulfilling the requirements for a Category-1 compacted backfill as specified by the United States Nuclear Regulatory Commission. In total, 25 lifts of compacted backfill were placed, and the as-built total thickness equaled 6.2 m. Lifts 1 through 13 made up the lower approximately 3 m of the test pad which was mainly silty sand (SP-SM) with some clayey sand (SP-SC and SW-SC) layers. Somewhat coarser sand (SP) with less fines (2.4 %) was placed in Lifts 14 through 25 which made up the upper approximate 3.2 m of the test pad. The average Proctor compaction levels of the lower and upper portions of the granular backfill were 103 and 101 %, respectively (Stokoe et al, 2018).

The shear wave velocities determined using the SABW method in the compacted backfill test pad site are shown in Figure 10 with star symbols. The frequency range of interest to investigate the dispersion of the shear wave was  $\pm 5$  % of the frequency of the local maxima.

The shear wave velocities calculated from the SABW and the conventional time-domain method show a gradually increasing trend of the shear wave velocity with depth as expect, and the values are close to each other. The dispersion of the shear wave was not significant.

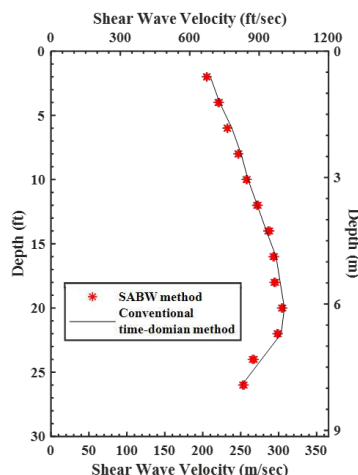


Figure 10. Shear wave velocities calculated from the SABW method and conventional time-domain analysis method in the compacted backfill test pad site

The crosshole test was performed at the Hornsby Bend Research Site as a part of developing work associated with the SABW method. The shear wave velocities determined using the SABW method at the Hornsby Bend Research site is shown in Figure 11 with the star symbols. As done with the compacted backfill test pad site, the frequency range of interest was  $\pm 5$  % of the frequency of the local maxima.

The shear wave velocities calculated from the SABW and the conventional time-domain method identify the two different velocity layers and the transition layer at the depths of 6 to 9 m. The shear wave velocity values are close to each other. The dispersion of the body wave is recognizable at the depths of 2.7 and 4.7 m which indicates the irregular shape of the waveforms.

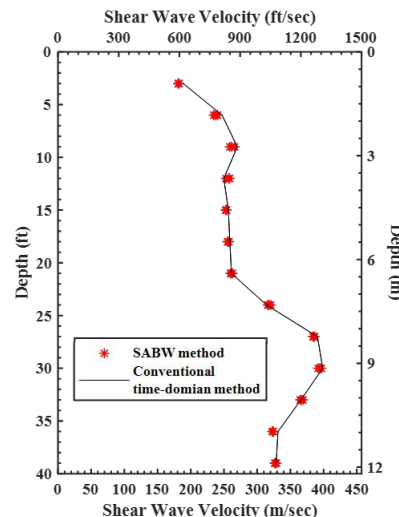


Figure 11. Shear wave velocity calculated from the SABW method and conventional analysis method in the Hornsby bend site

## 6 CONCLUSIONS

A reliable framework to calculate correct body (P- and S-) wave velocity using the SABW method is discussed herein. The SABW method is verified using synthetic waveform, laboratory experiment and field seismic test comparison. The wave velocity calculated from the SABW method shows stable values with lower variance compared to the conventional time-domain method. The framework can be easily coded which can remove the subjectivity and effort in visual selection of the arrival times and enables the investigation of dispersion in the body waves and, in the future, the attenuation of body waves for in-situ material damping measurement.

## 7 REFERENCES

- Hwang S. 2018. Advanced data analysis techniques for downhole seismic testing. *Geotechnical Engineering, Dept. of Civil, Architectural and Environmental Engineering*, Univ of Texas at Austin.
- Joh S.H. 1996. Advanced data analysis techniques for downhole seismic testing. *Geotechnical Engineering, Dept. of Civil, Architectural and Environmental Engineering*, Univ of Texas at Austin.
- Kim C.Y. 2012. Development of the Spectral-Analysis-of-Body-Waves (SABW) method for downhole seismic testing with boreholes or penetrometers. *Geotechnical Engineering, Dept. of Civil, Architectural and Environmental Engineering*, Univ of Texas at Austin.
- Meyer F. 1994. Topographic distance and watershed lines. *Signal Processing*, Vol. 38, 113-125.
- Robertson P. K., Campanella R. G., Gillespie D., and Rice A. 1986. Seismic CPT to measure in-situ shear wave velocity. *J. Geotech. Eng.*, 12(8), 791-803.
- Stokoe K. H. II. and Hoar R. J. 1978. Field measurement of shear wave velocity by crosshole and downhole seismic methods. *Proc. Conf. on Dynamical Methods in Soil and Rock Mechanics*, Vol. 3, Karlsruhe, Germany, 115-137.
- Stokoe K. H. II. and Woods R. D. 1972. In situ shear wave velocity by cross-hole method. *J. Soil Mech. Found. Div.*, 98(5), 443-460.
- Stokoe K. H., Hwang S., Boone M., Lewis M. R., Wang Y., Cooke M. F., and Keene A. K. 2018. Measured and Predicted Vs Values of a Granular Backfill Test Pad. *Proc. Conf. on Geotechnical Earthquake Engineering and Soil Dynamics V*, ASCE, GSP 293, Austin, Texas, 473-488
- Stokoe K.H. II., Hwang S.K., Roesset J.M., and Sun W.S. 1994. Laboratory measurements of small-strain material damping of soil using the free-free resonant column. *Proc. Earthquake Resistant construction and Design*, ERCAD, Berlin, 195-202.
- Woods R. D. 1978. Measurement of dynamic soil properties. *Proc. Conf. on Earthquake Engineering and Soil Dynamics*, ASCE, Vol. 1, Pasadena, CA, 91-178